CHAPTER 5

A hybrid deep learning approach to complete quantitation of proton magnetic resonance spectral peaks of the brain

Chapter highlights

- ***An attempt to utilizing wavelet feature descriptors and trainable convolutional feature in an ensembled hybrid learning model***
- ***Design an efficient overall analysis and quantitation model for MR spectra.***

1.1. Introduction

Magnetic resonance spectroscopy/spectroscopic imaging (MRS/MRSI) is a powerful technology used to study the chemical composition and metabolism of tissues in a variety of scientific and medical domains. It reveals important information on molecular structures, concentrations, and interactions in biological systems by measuring the signals emitted by specific metabolites, helping researchers and physicians to obtain insights into the biochemical composition and metabolic activities that occur in the brain *in-vivo* non-invasively, hence often termed as 'virtual biopsy.' Quantitation of biochemical entities is the main goal of MRS acquisitions to obtain the concentrations, ratios, and changes in these metabolites providing important information on brain function, metabolism, and diagnosing the underlying mechanisms of different neurological and psychiatric illness. In clinical MRS, time-domain acquisitions, also called free induction decay (FIDs), are obtained to map individual biomarkers in organs of interest to quantify for further analysis. At short echo times (TEs), MR acquired spectra have an immense baseline influence, contributed mostly by macromolecules (MMs), superimposed over metabolite spectra. In recent studies, it has also been inferred that MMs are

associated with potential pathological alterations in brain disease conditions like tumor, multiple sclerosis, and stroke, and some relevant information might get ignored by discarding these details [1-9]. In addition, clinical strength MR spectra have low SNR, linewidth issues, and artifacts associated, making the process of quantification difficult.

Quantitation can be approached in many ways, of which, the curve-fitting approaches to map individual components has been an established strategy. Different parametric and non-parametric model approaches have been developed to perform analysis and obtain spectral parameters from data, either in time-domain or frequency domain [10-18]. Similarly, machine/deep learning approaches have been implemented in a variety of tasks [19-20], and in recent years, MRS domain. Das et al. [21], Hatami et at. [22] proposed a multi-layer perceptron (MLP) and CNN network respectively for metabolite concentration estimation. Gurbani et at. [23] proposed an unsupervised convolutional encoder-model decoder approach to accelerate spectral fitting of whole brain MRSI spectra. Kyathanahally et al. [24] proposed a convolutional neural network (CNN) for ghosting artifact detection and removal. Gurbani et al. [25] developed CNN architectures for overall quality assessment of MR spectra based on artifacts present and spectral fitting. Lee et al. [26] designed a CNN network for spectral fitting and metabolite peak estimation. For correcting frequency and phase of acquired MR spectra, Ma et al. [27] came up for a convolutional neural network-based approach. Similarly, to address the issues of noise degradation of MR spectra, Lei et al. [28] used a stacked auto-encoder (SAE) model. Hu et al. [29] and Dandil et al. [30] proposed LSTM based designs to address the issues of noise, and grading of brain tumors, respectively.

The standard curve-fitting approaches lacks in scalability factor and capturing inter-spectral information especially when spectral data size is large and multiple voxels have been used from an ROI to obtain spectra, like MRSI acquisitions for tumor area localization. Machine/Deep learning approaches can counter these issues by handling multiple spectra at once, at the same

time learning inter-spectral relationships which can help in mitigating voxel contamination, residual peak analysis etc. Recent ML/DL approaches have addressed these issues as mentioned but, in most studies, the focus has been on metabolite estimation, discarding MM information as spectral baseline along with noise and artifacts, which can have possible diagnostic information and necessary for MRS as a diagnostic tool in a clinical setup.

In the present study, a hybrid inception-UNet architecture combined with fully connected dense layer regression block has been proposed in an attempt for overall relative peak quantitation of ^{1}H-MRS spectra, simulated in accordance with parameters of generic *in-vivo* brain spectra and *in-vivo* spectra, addressing both metabolites and MM components. This method is implemented in two steps: first, metabolite/MM isolation from noisy, degraded spectra and then regression for peak estimation.

1.2. Methods

1.2.1. Data augmentation and preparation

For training and testing data simulation, first, a basis-set of 18 individual metabolites [alanine (Ala), aspartate (Asp), creatine (Cr), ɣ-aminobutyric acid (GABA), glucose (Glc), glutamine (Gln), glutamate (Glu), glycerophosporylcholine (GPC), glutathione (GSH), lactate (Lac), myo-inositol (mI), N-acetylaspartate (NAA), N-acetylaspartylglutamate (NAAG), phosphorylcholine (PCho), phosphorylethanolamine (PE), phosphocreatine (PCr), taurine (Tau)] were obtained from source in [31]. The relative amplitude range for each metabolite was determined from the literature [26, 32-34]. Next, a basis-set for 17 MM components of Voigt lineshape were simulated with amplitude, linewidth and chemical shift parameters obtained from literature [1, 18, 26]. Then, an in-house augmentation module was designed in Spyder package (Python version 3.9; Python Software Foundation) to generate 30000 simulated spectra with the intent to mimic an *in-vivo* brain MRS spectra, as close as possible, by using a

linear combination approach. Finally, the simulated dataset was divided into training, validation, test sets in the ratio of (70/15/15) % for model training and further analysis.

To maintain variation in data and reduce any bias, specific measures have been taken and the steps to generate simulated train/validate/test dataset mimicking *in-vivo* brain spectra can be summarized as:

Step 1: Basis-set of individual metabolite peaks were obtained (ISMRM data challenge, 2016) [31], and normalized.

Step 2: For each 18 metabolites basis, relative concentration ranges (upper and lower bounds) were determined according to literature (See Appendix Table 1). These individual peak ranges were evenly divided into 10 values.

Step 3: The ground truth simulated spectra (N = 30000) were prepared by randomly selecting individual metabolite peak concentrations and adding together.

Step 4: Basis-set for 17 individual macromolecules (MM) were generated using Gaussian model functions and amplitude, linewidth, chemical shift parameters reported in literature (See Appendix Table 2).

Step 5: Spectral baseline signals (M = 30000) were generated by randomly selecting individual MM basis and adding together.

Step 6: To mimic *in-vivo* brain spectra, the metabolite and MM baseline were randomly selected and added together in the ratio [MM = (0.7 to 0.8) * metabolite].

Step 7: Simulated spectra obtained from step 6 were (a) individually line broadened by randomly using a value between 5-10 Hz, (b) frequency and phase shift introduced by ±10 Hz and ±2° respectively.

Step 8: All simulated spectra were Fourier transformed and final shape of all simulated spectra was set to (1024x1).

Step 9: Finally, random noise was added to each individual spectra to achieve SNR between 5-20 db for the dataset.

Note: Corresponding ground truth spectra in the dataset was curated without data augmentation steps 7, 9.

The relative amplitude and linewidth for individual metabolite and MM basis were varied and randomly combined with the idea to comprise the possible variabilities of healthy and/or pathological spectra mimicking *in-vivo* acquisitions.

1.2.2. Model architecture

The overall model architecture for this study derives its propositions from DTCWT decomposition [35], UNet networks [36], inception networks [37], residual networks [38], attention mechanism [39] and FCN-CNNs for curve fitting (to isolate metabolite and MM spectra) and regression tasks (for individual metabolite/MM peak estimation). The proposed architecture has two blocks: a modified backbone structure of a one-dimensional (1D) UNet where each module in encoder-decoder part is replaced with an inception module (1D) for fitting of noisy spectra to isolate metabolite-MM spectra separately, and a four-layer dense network as a regression block for individual relative peak amplitude estimation from isolated metabolite and MM spectra. The elements used in the proposed architecture are: (i) Wavelet transform: it is a powerful multi-scale signal analysis tool which decomposes a signal into its component features of varied resolution by scaling and shifting a localized-support mother wavelet function. For this study, dual tree complex wavelet transform (DTCWT) was used to decompose the spectra into approximation and detailed feature coefficients. Approximation features of training spectra with a multiplier of k=0.8 was used as residual connection. (ii) U-

Net backbone: U-Net is a convolutional neural network (CNN) architecture that was introduced in 2015 for biomedical image segmentation. It is named "U-Net" due to its U-shaped architecture, which consists of an encoder path (captures the context and extracts high-level features from the input image) and a decoder path (upsamples the feature maps to the original input resolution by using transposed convolutions (also known as deconvolutions or upsampling). In our proposed architecture, 4 encoder-decoder modules are taken and modified for this task. (iii) Inception module: Inception network, also known as GoogLeNet, was introduced by researchers at Google in 2014 to address some of the limitations of traditional CNN architectures, such as the problem of vanishing gradients and the high computational cost of deeper networks. In the present model, the convolutional modules of UNet model were replaced with inception modules having 1D convolutional blocks of kernal sizes of 1, 3, 5. The number of 1D convolutional filters used in the first inception modules were 16, 24, 24 and were doubled in subsequent 3 encoder inception modules. (iv) Residual connection: Residual Network, also known as ResNet, is a deep convolutional neural network architecture that was introduced in 2015 to address the problem of vanishing gradients in training very deep neural networks. In this context, inspired with ResNet architecture, a wavelet residual connection was incorporated in the 1st inception module and a traditional residual connection in the rest.

The two different variants of individual inception module design have been presented in the Figure 1. The design and training parameters for the inception modules have been presented in Table 1.

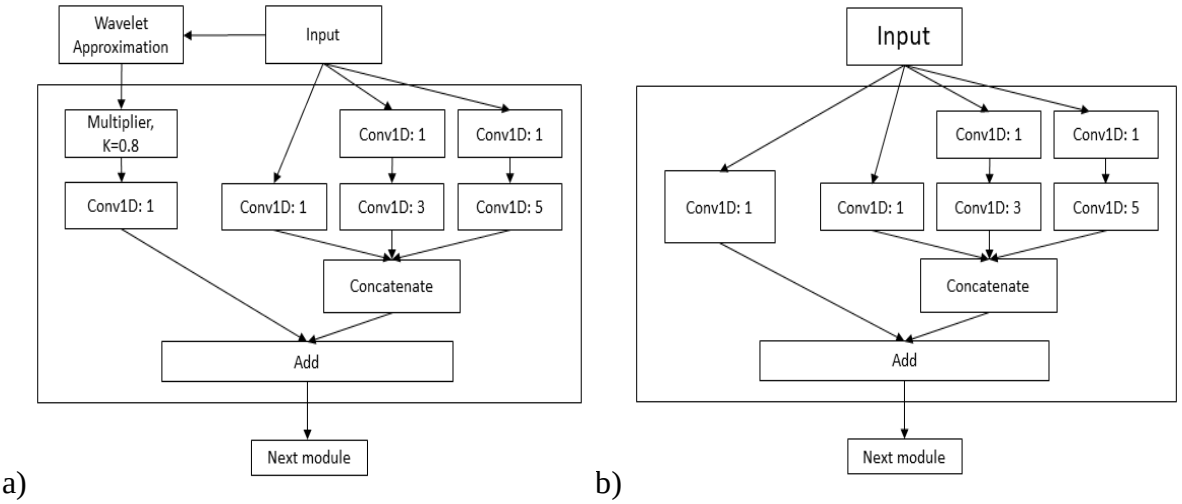

Figure 5.1: Inception module architecture for UNet encoder-decoder. (a) Wavelet residual inception module (used as 1st encoder block only), (b) Residual inception module for the rest encoder-decoder module.

To reduce the training computation time of the proposed architecture, the ability of 1x1 conv blocks was leveraged for the reduction of dimensions of the inputs passed through the inception module filters to reduce the number of multiplier operations.

Finally, two 4-layer dense network as regression model for individual peak estimation was used where both take input from last decoder inception module which has same shape as input (1024), and the output layer shapes are 18 for metabolite peak and 17 for MM peak estimator dense network. The hidden 3 dense layers have 512, 256, and 64 neurons in them. The overall schematic of the proposed model architecture is shown in Figure 2.

Table 5.1: Design and training parameters for inception modules used

1st Inception module parameters	**Values**
Input/Output shape	1024/1024
Wavelet/scale	DTCWT/Approximation [35]
Filter sizes in parallel (no. of filters)	1(16), 3(24), 5(24)

Residual connection/no. of filters	Wavelet approx*0.8/64
Kernal initializer	HeUniform
Kernal regularizer	L1: 1e-5, L2: 1e-4
Loss function	Mean Squared Error
Metric	Accuracy
Optimizer	ADAM [40]
Learning rate	0.25*1e-4
Batch size	32
No. of epochs	300
Activation function	Relu

In the present study, the problem of MRS spectra quantitation was divided into two steps: isolation of noise-free, corrected metabolite and MM spectra from degraded MRS spectra, and then, individual peak estimation. The first issue of metabolite-MM spectra isolation was addressed with the proposed inception-UNet architecture where it was trained in a supervised manner with simulated degraded training data set and concatenated ground truth metabolite-MM spectra and, the validation and test sets were used for model optimization and performance evaluations. This approach can be considered as an analogue of curve-fitting approach applied in deep learning domain with the advantage of highly scalable data processing at once as well as learning inter-dependent features among different spectra, if present. The training parameters for isolation purposes have been given in Table 1, where 'mean-squared error (MSE)' was used as objective loss function and 'accuracy' was used as a metric for isolation efficiency of the proposed model into metabolite class and MM class of spectra. The values of L_1- and L_2-regularizers, learning rate parameters were obtained by optimizing the inception-UNet part using parameter gridsearch over a range of values for each parameter to achieve the

lowest root mean-squared squared error (RMSE) value. In addition, Structural similarity index (SSIM), as an objective measure, was used to calculate the structural quality of predicted signals after processing compared to the ground truth spectra.

1.3. Results

For training the proposed model to obtain metabolite and MM spectra, 21000 spectra were randomly selected, 4500 spectra each as validation and test sets. The performance of the proposed approach was evaluated based on two criteria: metabolite-MM isolation from variable SNR simulated noisy MRS spectra and, relative peak amplitude estimation efficiency.

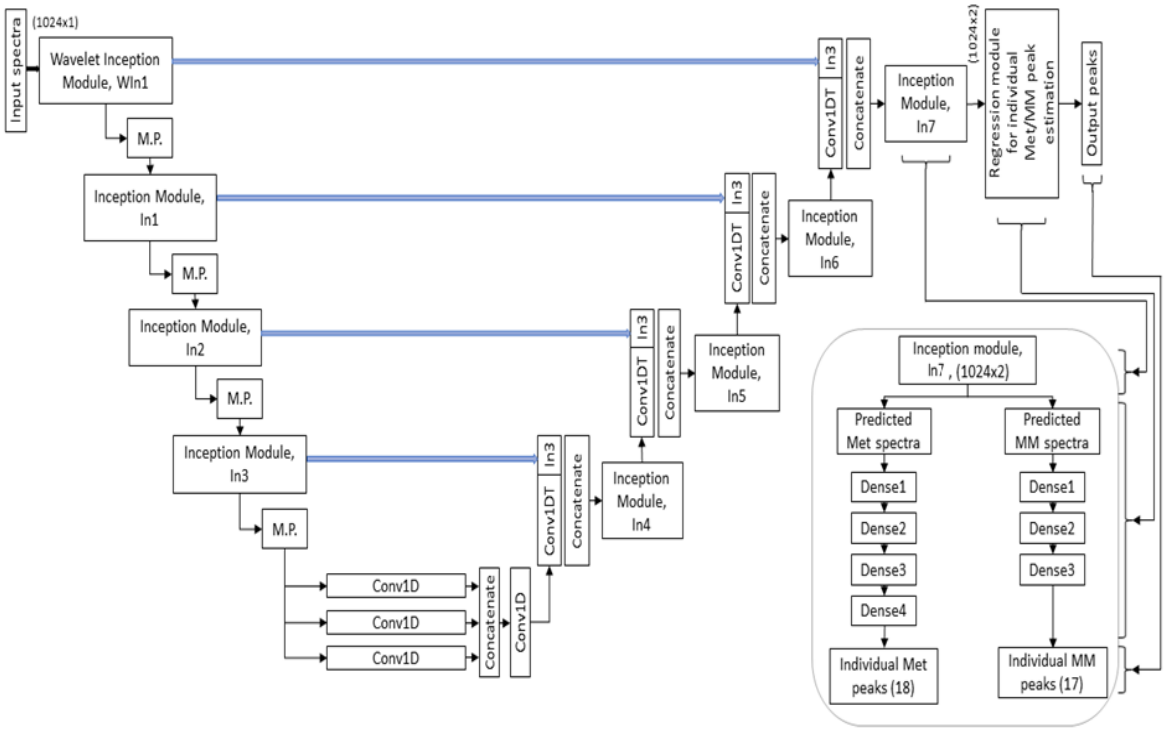

Figure 5.2: A schematic of the proposed model architecture for quantitation of MRS spectra.

1.3.1. Metabolite-MM isolation from spectra with different SNR

The noise degraded spectra with different SNR were divided into training, validation, and test sets. To investigate and compare the proposed model performance, individually optimized

standard UNet, UNet with attention module, and Attention-Residual UNet, and standard Inception UNet models were also trained on the same dataset. Mean-squared error ('mse') with L_1- and L_2-regularization was used as the objective loss function for training the model and accuracy as the evaluation metric for the overall performance evaluation of the isolation model (Figure 5.2). To further assess the model performance and compare with other equivalent models for the metabolite-MM isolation, RMSE value and SSIM were used as the statistical measures over the predicted spectra, where RMSE is a measure to show the amount of deviation of residual error between original and predicted signal. It is calculated as: $RMSE = \sqrt{\frac{\sum_{i=1}^{N}(x_i - \tilde{x})^2}{N}}$, where x_i is the original signal and $\tilde{x}$ is the predicted signal,

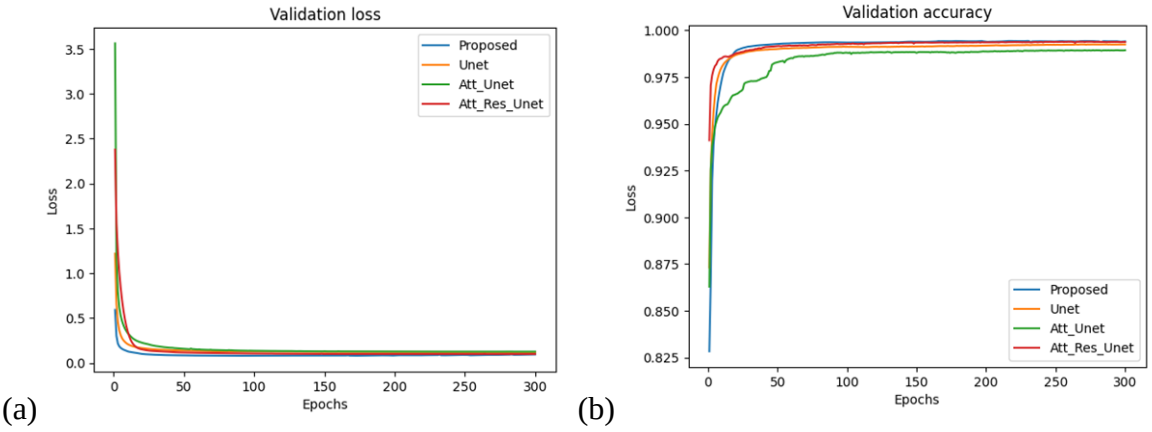

(a) (b)

Figure 5.3: Comparative plots of the trained model performance: (a) loss function: mse (b) metric: accuracy

SSIM is calculated as: $SSIM\ (X,Y) = \frac{(2\mu_X\mu_Y + c_1)(2\sigma_{XY} + c_2)}{(\mu_X^2 + \mu_Y^2 + c_1)(\sigma_X^2 + \sigma_Y^2 + c_2)}$, where predicted signal is represented as X and ground truth signal as reference signal Y; $\mu_X\ and\ \mu_Y$ are the mean and σ_X and σ_y are the standard deviation of X and Y respectively; σ_{XY} is covariance of X and Y; $c_1$and c_2 are stabilizing constant term, each for mean and standard deviation. The performance of the proposed model over spectra of different SNR in metabolite-MM isolation is presented in Figure 5.3 and the comparative performance evaluation metrics is given in Table 5.2.

Table 5.2: Comparative performance outcomes of the trained models

Met/MM isolation module	Validation loss	Test RMSE	Accuracy	SSIM (metabolites) value ± std	SSIM (MM) value ± std
UNet	0.0794	0.2774	0.9824	0.8999±0.0399	0.9111±0.0209
Attention UNet	0.0856	0.2887	0.9793	0.8831±0.0348	0.8923±0.0201
Attention ResUNet	0.0785	0.2770	0.9837	0.9370±0.0194	0.9432±0.0095
Inception UNet	0.0846	0.2853	0.9845	0.9214±0.0354	0.9372±0.0214
Proposed	**0.0714**	**0.2684**	**0.9919**	**0.9427±0.0243**	**0.9506±0.0271**

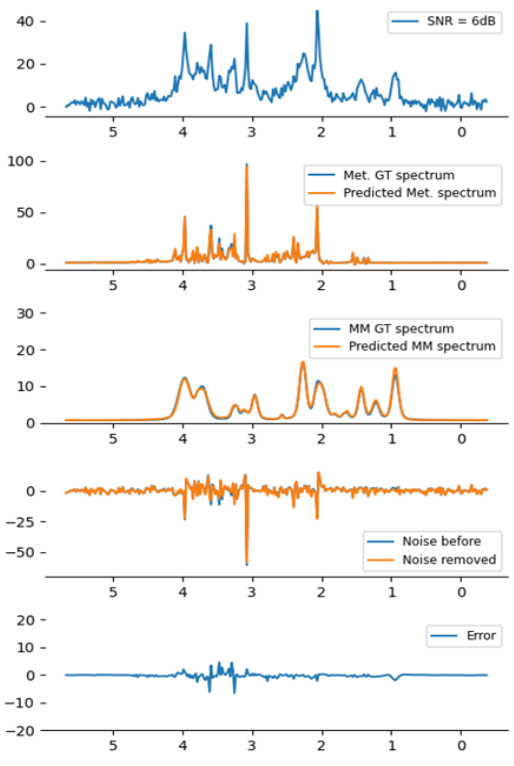

(a)

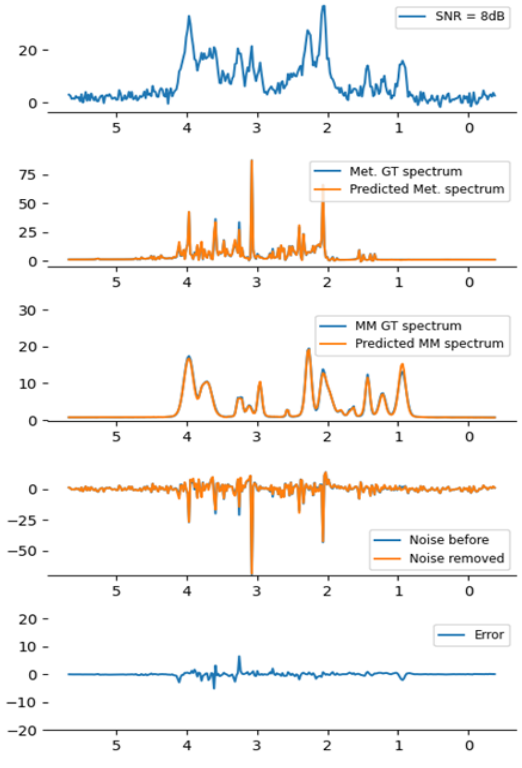

(b)

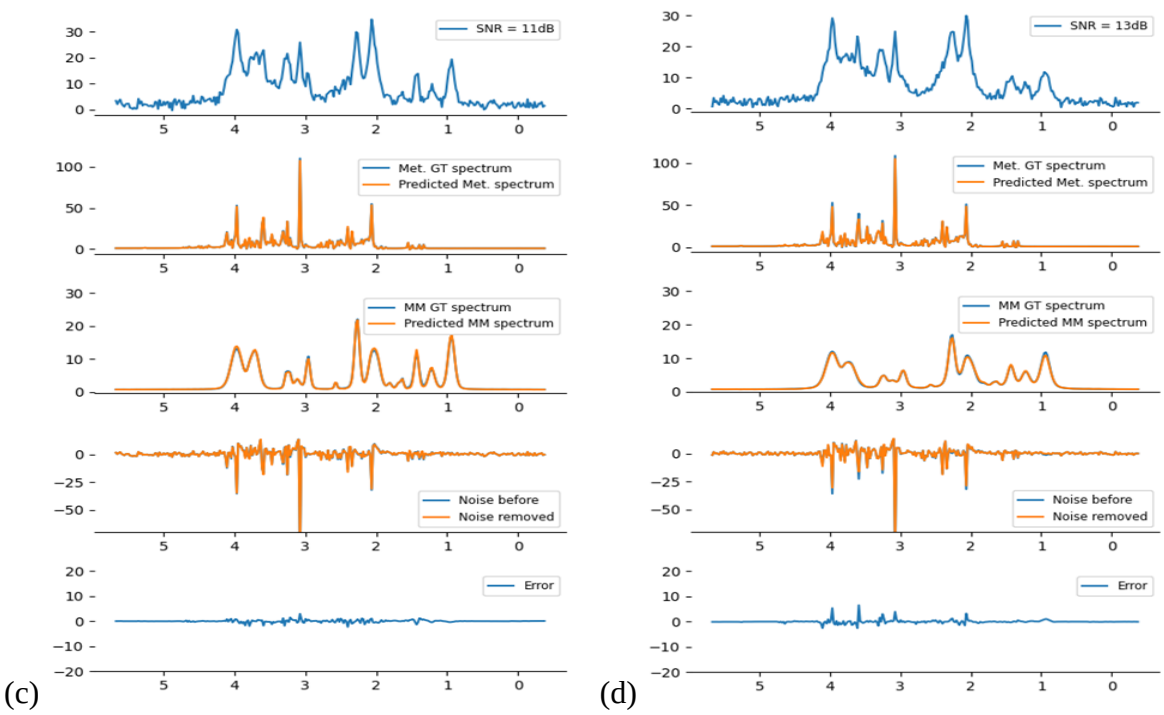

(c) (d)

Figure 5.4: Isolation of Metabolites and MMs from simulated test set brain MR spectra with different SNR: (a) 6 db, (b) 8 db, (c) 11 db, (d) 13 db. Each plot has five subplots: Noise degraded spectrum, overlapped ground truth and predicted metabolite spectra, overlapped ground truth and predicted MM spectra, overlapped noise added and noise removed, error between ground truth, and predicted (Met+MM) spectra.

The models were implemented in Colab Jupyter noteboob by Google Inc. [41] and trained on its GPU with Intel Xeon CPU @2.20 GHz, 13 GB RAM, Tesla K80 accelerator, and 12 GB GDDR5 VRAM. The run times for each model over (training + validation set) spectra are: (i) standard UNet: 1:16:27.929 hr, (ii) Attention UNet: 1:36:35.379 hr, (iii) Attention Residual UNet: 1:41:43.168 hr, (iv) Inception UNet: 1:40:17.926 hr, (v) Proposed: 1:41:49.278 hr.

1.3.2. Relative peak amplitude estimation

In time-domain MRS, individual metabolite/MM peak amplitudes are directly proportional to their relative concentration in the acquired FIDs. Peak heights/amplitudes, as well as their ratios, have been utilised as metrics for relative quantification of metabolites, as well as

classification and assessment in brain-related pathologies. Obtaining peak data from individual MM components will aid in further quantification and disease-specific analysis.

A regression-dense layer module was used to obtain amplitude estimates of individual peak components from the isolated metabolite and MM spectra separately. Table 5.3 presents the performance evaluation results of the module, where 'mse' was used as the objective loss function and RMSE was used as the evaluation metric for overall model performance. A set of 10000 metabolite and MM spectra (5000 each) from the noise-removed model output were used where a ratio of 60/20/20 % was used as train/validate/test set during training and performance evaluation of this module. Figure 5.4 plots the estimated amplitude of individual metabolite and MM peaks along with their ground truth obtained from the average of 2000 isolated test spectra.

Table 5.3: Performance evaluators for the peak amplitude estimation

Regression module for peak estimation	**Validation Loss**	**Test RMSE**	**MAPE (%)**
Reg1Met	0.0327	0.0833	9.03
Reg1MM	0.0067	0.1807	4.09

For each metabolite/MM relative concentration or peak amplitude estimated, mean absolute percentage error (MAPE) was calculated. For all the 18 metabolites, the overall MAPE

calculated was 9.03 %, with Ala, GABA, PCho, and NAAG having highest MAPE at 9.14, 10.44, 11.07, and 9.91 % respectively. For GSH, Gly, and NAA, MAPE were 8.48, 8.60, 7.29 and for rest of the metabolites, MAPE was below 5%.

Similarly, for 17 estimated MM peak, the overall MAPE was 4.09% with $M_{1.22}$, $M_{3.27}$, $M_{3.79}$ having values above 5.5%. The rest of the MM peaks ranges between 2.21-3.9% of MAPE.

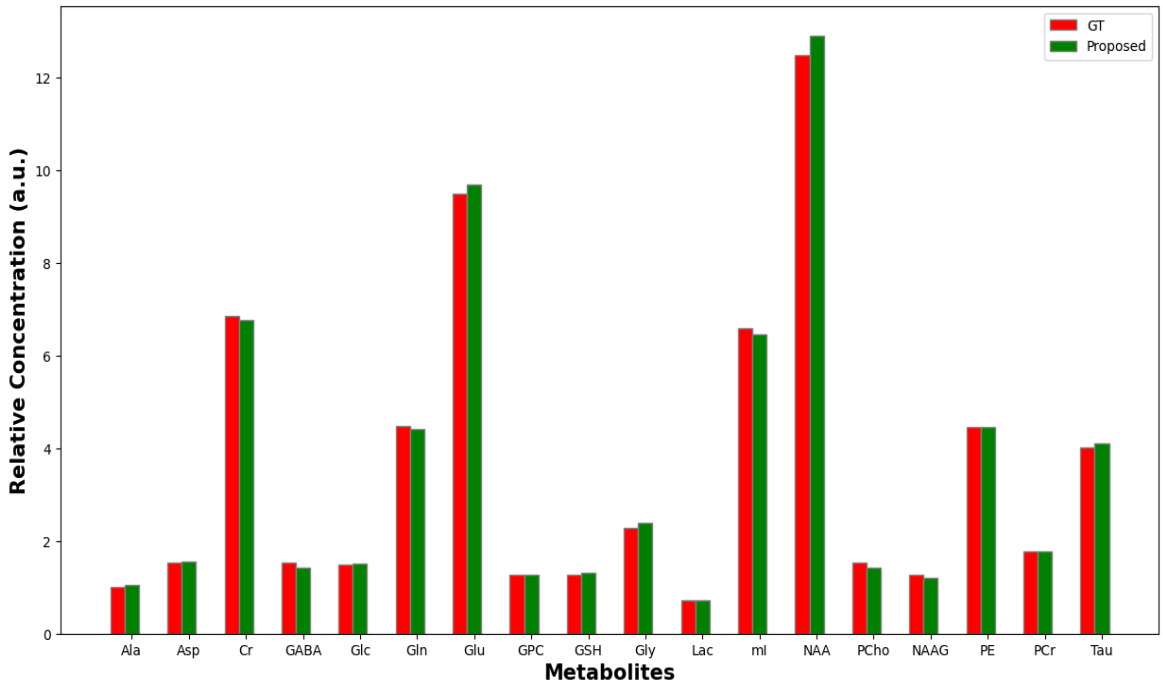

(a)

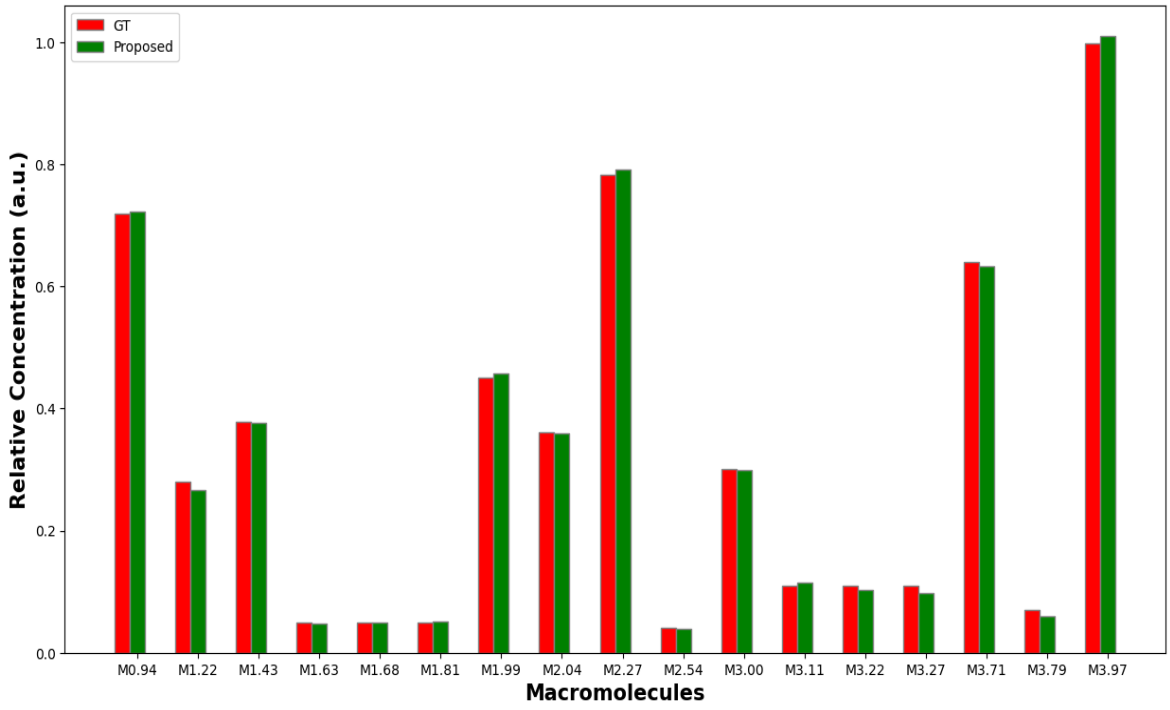

(b)

Figure 5.5: Combined plot of individual peak estimates (ground truth vs. proposed): (a) metabolite peaks, (b) MM Peaks. [a.u.: arbitrary units, used for relative concentration estimate).

Figure 5.5 presents the peak estimation outcomes of individual metabolite (5.5a) and MM (5.5b) components along with their respective ground truth values averaged over peaks from 4500 metabolite and MM spectra independently.

During data augmentation, the relative concentration range of each metabolite and MM component was divided into 10 equal parts to be used in a linear combination summation approach to obtain the ground truth spectra. In addition to the above statistical measures, and to gain more insights into the level of agreement, bias, and any potential systematic errors between the ground truth and proposed method, Bland-Altman (BA) plot [42] were generated for each metabolite and MM peaks (Figure 5.6).

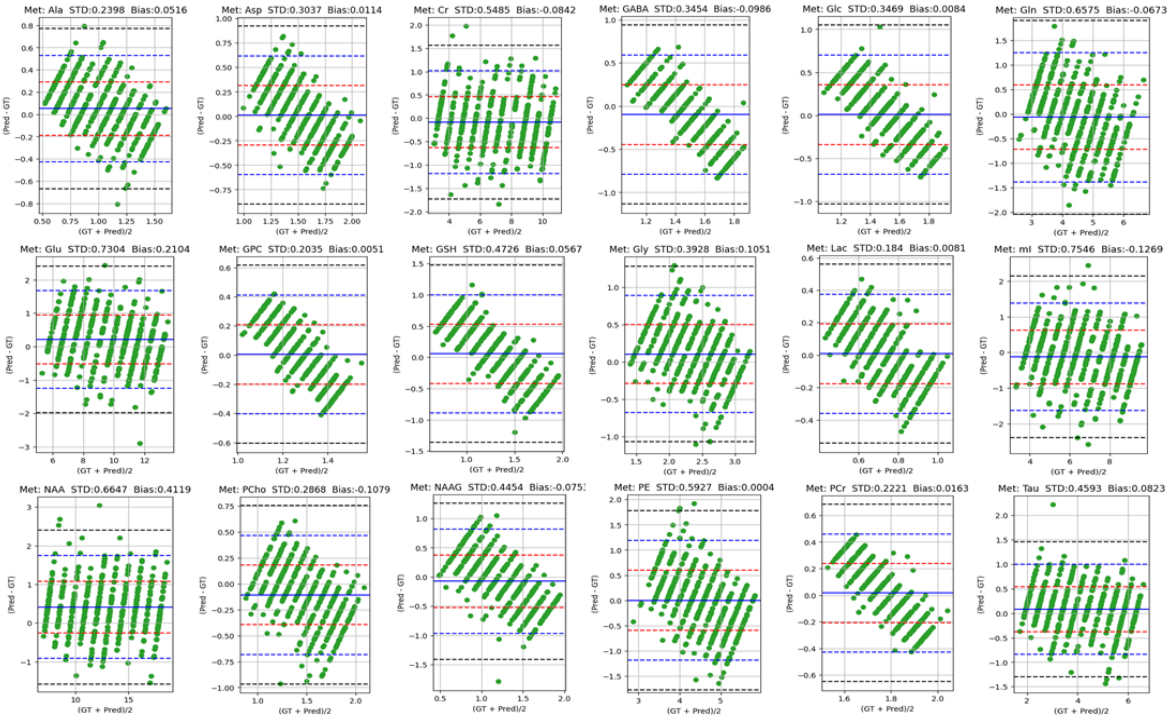

(a)

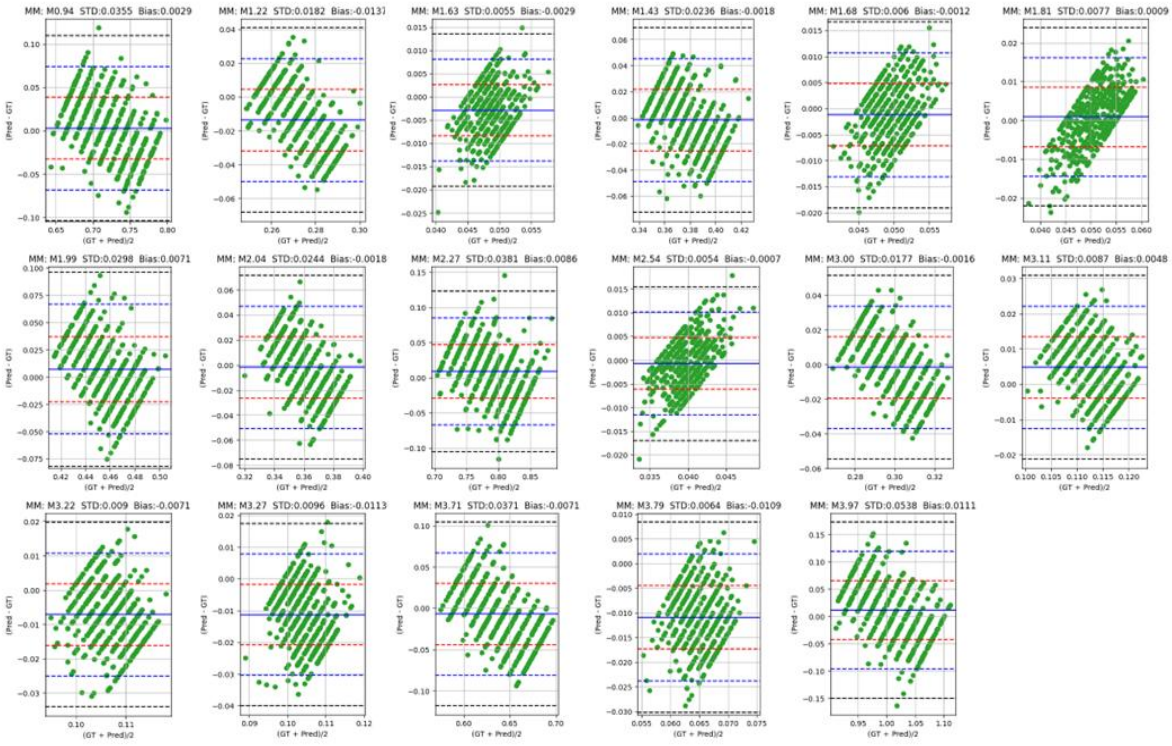

(b)

Figure 5.6: Bland-Altman plot of individual peaks. (a) for Metabolite (b) for MMs.

The figure 5.6 showing BA-plots for (a) individual metabolites, (b) MM components is essentially a plot of error *vs* mean between ground truth and predicted values. In each subplot, x-axis represents mean values (GT+Pred)/2, y-axis is error (Pred-GT), solid horizontal blue

line is mean error, dotted red lines are mean error±STD, dotted blue lines are error±2*STD, and dotted black lines are error±3*STD, the standard nomenclature, standard deviation, and bias for each peak is added to the title of each subplot.

From the plots, it can be inferred that each set of the 10 concentration values for the individual compounds has been isolated efficiently with the error within the limit of mean ± 2*STD suggesting faithful and robust model optimized for peak estimation of MRS data.

1.3.3. Residual water peak removal

The residual water peak in magnetic resonance spectroscopy (MRS) refers to the signal that remains after attempts to suppress or remove it from the water resonance during acquisition of *in-vivo* spectra. The presence of residual water peak in a noisy clinical spectrum further degrades its quality thereby making the interpretation and quantitation of MR spectra more challenging. It is, therefore, an absolute necessity to reduce the contribution of water peak in a spectrum as much as possible. In this study, residual water peaks of gaussian lineshape with linewidth in 35-45 Hz range were generated and centred between 4.6-4.8 ppm range. Since, the water suppression during acquisition brings down the residual water peak height in comparable range or some factor of metabolite peak height [43-45], the proposed model was trained and evaluated over the same dataset added with residual water peak amplitude in the range of (2-6) times the highest peak amplitude of the spectrum to consider for ineffective water suppression. The dataset was split into (70/15/15) ratio for the model performance evaluation.

The model was trained and evaluated with the same hyperparameters as mentioned in Table 1 to obtain the model performance results. Figure 5.7 shows the results of isolation of metabolite and MM spectra from degraded MR spectra superimposed with residual water peak and having SNR values of 5 db and 8 db. The model achieved an accuracy of 96.17% with the validation loss of trained model at 0.0934 in isolating the metabolite and MM spectra from the noise

degraded, residual water peak overlapped spectra. The RMSE, SSIM (metabolites) and SSIM (MM) values obtained for the test dataset were 0.3127, 0.9013, and 0.9131 respectively. The validation losses and RMSE values for the peak estimation module were 0.0809 and 0.2872 for metabolites, and 0.0222 and 0.1501 for MMs respectively. The overall MAPE for metabolite and MM peaks were 12.73% and 9.64% respectively.

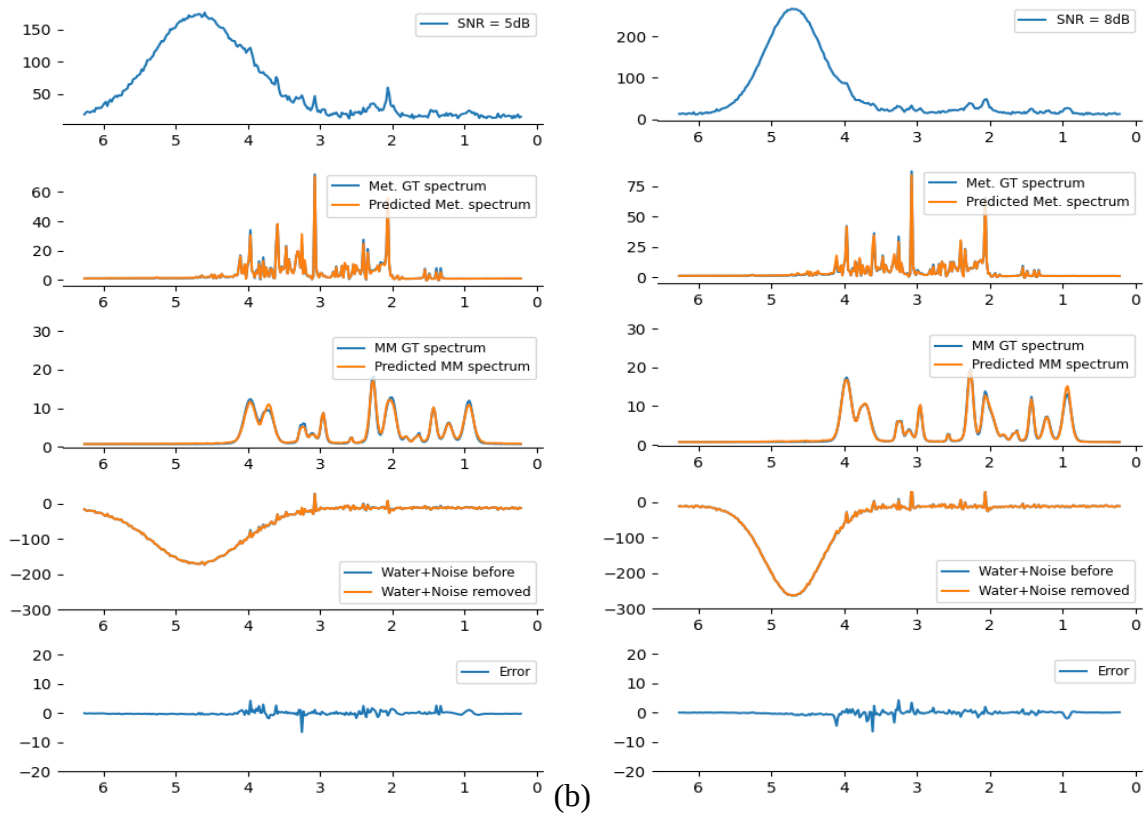

(a) (b)

Figure 5.7: Isolation of Metabolites and MMs from simulated test set brain MR spectra with residual water peak at SNR: (a) 5 db, (b) 8 db. Each plot has five subplots: Noise degraded spectrum with residual water peak, overlapped ground truth and predicted metabolite spectra, overlapped ground truth and predicted MM spectra, overlapped water + noise added and removed, error between ground truth and predicted (Met+MM) spectra.

1.4. Discussion

In clinical setting, an *in-vivo* brain ^{1}H-MRS acquisition from a subject is performed to study pathology and diagnosis. The acquired raw time-domain spectra obtained require

preprocessing, analysis steps for peak fitting before performing any quantitation estimation, relative or absolute, for a reliable, robust and generalizable assessment.

In the present work, the potential applicability of a deep learning approach for end-to-end ^{1}H-MRS spectral analysis was evaluated. A hybrid inception-Unet approach for spectral isolation was evaluated over spectra with varied SNR and line broadening. The predicted results indicates that the current method is particularly robust to noise present in the training spectra set. It achieved very high accuracy of 99.19% in isolating corrected metabolite and MM spectra from degraded acquisition while removing the noise components effectively.

For the estimated metabolite peaks of Ala, GABA, PCho and NAAG, MAPE was above 9% and for estimated MM peaks, the overall MAPE was above 5% for $M_{1.22}$, $M_{3.27}$, $M_{3.79}$. For rest of the metabolites and MMs, the estimation was below 9% of MAPE overall. These results are promising and better in comparison to previous attempts at MR spectra peak estimation and quantitation. Using an even larger dataset and/or including *in-vivo* dataset with a priori information of peaks during training the model is expected to further reduce MAPE making the quantitation process more accurate.

The presence of residual water peak in MR spectra is a major constraint in peak estimation as it corrupts the baseline around 3-5.5 ppm range overlapping the metabolite/MM peaks in that range. The performance of the model evaluated for metabolite-MM isolation was encouraging where the accuracy achieved was around 96% and, RMSE of 0.3127. The results are promising and minor adjustments in the model or incorporating some prior characterization of residual peak during training will further improve the outcome for spectra with even higher water residual peaks. Also, the proposed approach can further push for the quantitation of MR spectra from water unsuppressed acquisitions.

The idea behind using the approximation coefficients of wavelet transformed dataset as a residual connection was two-fold. First, the wavelet approximation features remove the high frequency noise presenting smooth representation of the original spectra. Also, DTCWT decomposition is approximately shift-invariant, the wavelet and scaling functions are approximately analytic with better directional selectivity, and less redundant compared to undecimated DWT. Secondly, features obtained by wavelet transform are static but interpretable unlike abstract and difficult to clearly understandable features produced by learned convolutional filters, and combining both feature types during training significantly improved the training and performance of the model over a test dataset (N=4500) which is completely independent of one another, and can introduce some interpretability factor to it.

Some of the limitations in our study are related to residual water peak-based evaluation, an incorporation of *in-vivo* dataset, for not just parameter tuning of the model, but into the fold for training and evaluation purposes as well. Introducing features from different wavelet scales has not been tried and may further improve the generalizability of the model for a diverse dataset.

1.5. Conclusions

The proposed deep learning hybrid approach to overall ^{1}H-MRS quantitation shows promise in robustness to noise variability in spectra, metabolite-MM spectral isolation, and efficient peak estimation for relative quantitation of both metabolite as well as macromolecular peaks at the same time. This may further the potential of using hybrid deep learning approaches in post-acquisition ^{1}H-MRS spectral analysis.

Appendix

- **Appendix Table 1: Relative metabolite concentration range used in current study for the individual basis in simulating the brain spectra (Small variations in values can be found in different literature)**

Metabolite basis	Chemical shift (main peak/multiplet) (ppm)	Concentration Range (mmol/L)
Ala	1.40	0.5-1.5
Asp	3.89	1.0-2.0
Cr	3.03	3.5-10.0
GABA	3.0	1.0-2.0
Glc	3.88, 5.22	1.0-2.0
Gln	2.2-2.4	3.0-6.0
Glu	2.2-2.4	6.0-12.5
Gly	3.55	1.0-1.5
GPC	3.2	0.5-2.0
GSH	2.15, 2.55, 2.93, 2.98, 3.77, 4.56	1.5-2.0
Lac	1.31	0.4-1.0
mI	3.52	4.0-9.0
NAA	2.01	7.5-17.0
NAAG	2.04	1.0-2.0

PCho	3.2	0.5-2.0
PCr	3.03	3.0-5.5
PE	3.22, 3.98	1.5-2.0
Tau	3.25, 3.42	2.0-6.0

- **Appendix Table 2: Parameters used to generate Macromolecular spectral baseline (expected at B_0 = 3T). (Small variations in values can be found in different literature)**

MM peak, M_{xx}	Chemical shift (in ppm)	Mean Amplitude (Normalized to peak amp at $M_{3.97}$)	Mean linewidth (in Hz)	Probable MM component
$M_{0.94}$	0.94	0.72	25.20	Leucine, isoleucine, valine
$M_{1.22}$	1.22	0.28	21.10	Threonine
$M_{1.43}$	1.43	0.38	15.90	Alanine
$M_{1.70}$	1.63	0.05	7.50	Lysine, arginine, leucine
	1.68	0.05	13.0	
	1.81	0.05	13.0	
$M_{2.05}$	1.99	0.45	29.03	Glutamate, glutamine
	2.04	0.36	20.53	
$M_{2.27}$	2.27	0.78	17.89	Glutamate, glutamine
$M_{2.54}$	2.57	0.04	5.30	β-methylene protons of aspartyl groups
$M_{3.00}$	3.00	0.30	14.02	Lysine
	3.11	0.11	17.89	Valine-H_β,

$M_{3.21}$	3.22	0.11	10.0	αCH protons of protein amino acids
	3.27	0.11	10.0	
$M_{3.71}$ + $M_{3.79}$	3.71	0.64	33.52	αCH protons of protein amino acids
	3.79	0.07	11.85	
$M_{3.97}$	3.97	1.0	37.48	

Publication out of this study: (In communication/review)

A hybrid deep learning approach to complete quantitation of proton magnetic resonance spectral peaks of the brain

(Quantitation of 1H-MRS with deep learning)

Chiranjeev Sagar[1*], Deepak Kumar Singh[2], Neeraj Sharma[1]

[1] School of Biomedical Engineering, Indian Institute of Technology (BHU), Varanasi, Uttar Pradesh, India

[2] Department of Oncology, Apex Super-speciality Hospital and Post Graduate Institute, Varanasi, Uttar Pradesh, India

Email(s): chiranjeevs.rs.bme16@iitbu.ac.in; deepakbhu@gmail.com; neeraj.bme@iitbhu.ac.in